

# A SPONTANEOUS GENERATION OF THE MAGNETIC FIELD AND SUPPRESSION OF THE HEAT CONDUCTION IN COLD FRONTS

Nobuhiro OKABE and Makoto HATTORI

*Astronomical Institute, Tohoku University, Sendai 980-8578, Japan*

okabe@astr.tohoku.ac.jp

hattori@astr.tohoku.ac.jp

## ABSTRACT

We have determined the physical mechanism responsible for the plasma instabilities, which was first found by Ramani and Laval (1978), associated with anisotropic velocity distributions induced by the temperature gradient in which there are growing low frequency transverse magnetic waves, even in the absence of background magnetic fields. We have shown that the physical mechanism responsible for the growth of one of the modes is identical to the Weibel instability. The nonlinear saturation level of the instability is also provided by considering the wave-particle interactions. The non-linear evolutions of the magnetic fields after the saturation are speculated. The results are applied to the cold fronts which is one of the newly discovered structures in clusters of galaxies by the Chandra X-ray observatory. We predict the existence of the magnetic field of  $\sim 10\mu\text{G}$  tangential to the surface over the entire region of the cold front surface and that the heat conduction is significantly suppressed by the trapping of the electrons by the generated magnetic fields. The instability may provide a new possibility on the origin of cosmic magnetic field.

*Subject headings:* galaxies: clusters: general—magnetic fields—conduction—instabilities—plasmas

## 1. INTRODUCTION

The Chandra X-ray observatory revealed the bow-shaped discontinuities in the X-ray emitting hot plasmas in the clusters of galaxies (Markevitch et al. 2000). The plasma temperature sharply increases across the discontinuities, while the plasma density sharply decreases across the discontinuities toward the same direction. These new structures are called

cold fronts. The cold fronts might be the contacting surfaces of two different origin plasmas. If the classical Spitzer heat conductivity is applied, the life time of the cold fronts should be  $\sim 10^6$ yr. Since it is much less than the expected ages of the cold fronts, that is  $> 10^8$ yr, the heat conductivity in the cold fronts region must be significantly reduced from the classical Spitzer value (Ettori & Fabian 2000; Markevitch et al. 2000). Since there are thermal pressure jumps across the fronts (Vikhlinin, Markevitch & Murray 2001a), a transonic motion of the cold fronts is expected to maintain the pressure balance between the cold and hot regions. Vikhlinin et al. (2001b, 2002) pointed out that the magnetic field of  $10\mu\text{G}$  along the fronts should exist to explain the smoothness of the fronts otherwise the irregular structures are expected due to the Kelvin-Helmholtz (KH) instability. Since the required field strength is more than order of magnitude stronger than the intracluster magnetic field strength while the plasma density jump is at most factor of two across the cold fronts, the compression of the intracluster magnetic field as conserving the flux can not explain the existence of such a strong magnetic field in the cold fronts.

A precise mathematical treatment of the thin hot plasmas based on the plasma kinetic theory found that the anisotropic electron velocity distribution induced by the temperature gradient drives the plasma instability, and it is postulated that the electron scattering by the excited plasma waves may significantly reduce the heat conductivity (Ramani & Laval 1978). The low frequency transverse growing magnetic waves are excited even in the absence of an background magnetic field. Since the instability was found by Ramani and Laval (1978), the instability is referred to the Ramani-Laval (RL) instability in this paper. The applications of the RL instability to the cluster hot plasmas were examined by some authors; in cases of the plasma with background magnetic fields (Levinson & Eichler 1992) and the electron-ion two components plasma (Hattori & Umetsu 2000). Although the RL instability was said to be the Weibel like instability (Weibel 1959) since the growth of the waves is seeded by the anisotropic velocity distribution, there are plenty of the qualitative differences among the both instabilities as explained in section 3. Therefore, the both instabilities were distinguished (Gallev & Natanzon 1991) and it is very important to determine the physical mechanism of the RL instability.

Since this paper is the first paper of our series of papers, we focus on the identification of the physical mechanism of the RL instability (in §2. and 4.) including the review of the Weibel instability (in Appendix) and the RL instability (in §3), the determination of the non-linear saturation level of the excited waves and the non-linear evolution of the excited modes (in §5), and the application to the cold fronts (in §6.). Section 7 is devoted to discussion.

## 2. THE VELOCITY DISTRIBUTION FUNCTION IN THE PLASMA WITH THE HEAT FLUX

In this section, how the anisotropic electron velocity distribution function is set up when the temperature inhomogeneity exists in the plasma, is discussed from physical point of view. The absence of a background magnetic field is assumed. Consider the temperature inhomogeneity in hot electron plasma with the temperature variation scale of  $L$ . Since the heat conduction carries the heat flux from the hotter to cooler regions, the heat flux along the temperature gradient takes a negative finite value;  $q \propto \langle v_{\parallel} v^2 f \rangle < 0$  where the bracket denotes the integral over the velocity space and the subscript  $\parallel$  denotes the component parallel to the temperature gradient. Therefore, the electron velocity distribution function must deviate from the Maxwell-Boltzmann  $f_m = n_0(x_{\parallel})(\pi v_{\text{th}}(x_{\parallel})^2)^{-3/2} \exp(-v^2/v_{\text{th}}(x_{\parallel})^2)$ ;  $\Delta f = f - f_m \neq 0$ . Here,  $n_0(x_{\parallel})$  is the electron number density,  $v_{\text{th}}(x_{\parallel}) = (2k_B T(x_{\parallel})/m_e)^{1/2}$  is the thermal velocity with the temperature  $T(x_{\parallel})$  and the electron mass  $m_e$ . The above condition together with  $\langle \Delta f \rangle = 0$ , that is the number density conservation, and  $\langle v^2 \Delta f \rangle = 0$ , that is the energy conservation, restrict the form of the deviated part,  $\Delta f$ , to be odd function of the velocity component along the temperature gradient,  $v_{\parallel}$ . Of course,  $\Delta f \rightarrow 0$  as  $|v_{\parallel}| \rightarrow \infty$ . In Figure 1, the possible cases as  $\Delta f$  are shown. From zero current condition, such as  $\langle v_{\parallel} \Delta f \rangle = 0$ , the form like the type A is rejected since  $\Delta f$  where  $v_{\parallel} > 0$  and  $v_{\parallel} < 0$  are respectively positive and negative, and then  $v_{\parallel} \Delta f > 0$  for all velocity and  $\langle v_{\parallel} \Delta f \rangle > 0$ . On the other hand, the type B and C satisfy the zero current condition since  $\Delta f$  curve crosses the  $v_{\parallel}$ -axis in each positive and negative  $v_{\parallel}$  region. The  $\langle v_{\parallel} v^2 f \rangle$  for the type B and C have finite values because this is the weighted mean of  $\langle v_{\parallel} \Delta f \rangle$  weighted by  $v^2$  which is larger when  $|v_{\parallel}|$  is larger. The heat flux condition of  $\langle v_{\parallel} v^2 f \rangle < 0$  says that  $\Delta f$  where  $v_{\parallel} \rightarrow -\infty$  should be positive. Thus, the type C is only the possible form as the deviated part in the plasma where the finite heat flow exists. The relative amplitude of the deviated part to the Maxwell-Boltzmann should be  $\epsilon \delta_T$  where  $\epsilon = \lambda_{\text{mfp}}/L$  and  $\delta_T = \delta T/T$  is the fractional temperature fluctuation, since the deviation may be induced by the Coulomb collision and the temperature fluctuation.

The deviated part  $\Delta f$  can be also deduced analytically. The Boltzmann equation is

$$\frac{\partial f}{\partial t} + v_{\parallel} \frac{\partial f}{\partial x_{\parallel}} - \frac{e}{m} E_{\parallel} \frac{\partial f}{\partial v_{\parallel}} = -\nu(f - f_m),$$

where  $E_{\parallel}$  is the zeroth electric field along the temperature gradient and the rhs is the Krook operator as the collision term and  $\nu = (k_B T/m_e)^{1/2}/\lambda_e$  is the Coulomb collision frequency with the Coulomb mean free path  $\lambda_e$  (Sarazin 1988). Hereafter, we describe the collision frequency as  $\nu = v_{\text{th}}/\lambda_{\text{mfp}}$  with the parameters  $v_{\text{th}} = (2k_B T/m_e)^{1/2}$  and  $\lambda_{\text{mfp}} = \sqrt{2}\lambda_e$ . For simplicity, the pressure balance is assumed. Then,  $E_{\parallel} = 0$  (Ramani & Laval 1978). If the

perturbative treatment is applicable to describe the system, the distribution function could be expanded in  $\epsilon\delta_T$  (Chapman & Cowling 1960) as,

$$f = f_m + \epsilon\delta_T f^{(1)} + \epsilon^2\delta_T^2 f^{(2)} \dots,$$

where  $f^{(j)}$  ( $j = 1, 2 \dots$ ) describe the deviation of the distribution function from the Maxwell-Boltzmann in order of  $(\epsilon\delta_T)^j$ . This expansion is known as the Chapman-Enskog expansion. Therefore, the electron distribution function up to the first order in  $\epsilon\delta_T$  is obtained as

$$f = f_m \left[ 1 + \epsilon\delta_T \frac{v_{\parallel}}{v_{\text{th}}} \left( \frac{5}{2} - \frac{v^2}{v_{\text{th}}^2} \right) \right].$$

The form of the deviated part is essentially the same as the type C shown in Figure 1. We would like to note that adopting the Krook operator is not essential for determining the form of the deviated part.

### 3. THE REVIEW OF THE RL INSTABILITY

The diagnostics of the Ramani-Laval (RL) instability are summarized contrasting with the Weibel instability. As summarized in the Appendix, the temperature anisotropy excites the transverse magnetic waves due to the Weibel instability. The excited wave is standing wave with zero phase velocity. The amplitude of the wave grows when the temperature perpendicular to the wave vector is higher than the temperature parallel to the wave vector. The amplitude of the wave is damped in the opposite situation.

Ramani and Laval (1978) studied the stability of the plasmas when the temperature distribution is not homogeneous. The non-equilibrium electron velocity distribution function is deduced from the assumed temperature distribution self consistently using the Chapman-Enskog expansion. This is one of the prominent difference from the Weibel case where the anisotropic electron velocity distribution function due to the temperature anisotropy is given by hand. The difference of the deduced non-equilibrium velocity distribution function from the equilibrium one, that is the Maxwell-Boltzmann distribution, is skewed in the direction of the temperature gradient and is the odd function of the velocity component along the temperature gradient. The velocity distribution functions in the both cases are anisotropic. However, the skewed nature found in the RL case is not found in the Weibel. Although the anisotropic velocity dispersion is essential for the Weibel instability, the velocity dispersion is isotropic in the RL case. Ramani and Laval (1978) performed the linear stability analysis of the plasmas with the deduced non-equilibrium velocity distribution following the procedure of the plasma kinetic theory. Two independent modes appear. The two modes are distinguished

whether the magnetic field is in or not in the plane made by the temperature gradient and the wave vector, where the first one is named mode 2 and the second one is named mode 1. The dispersion relation of the both modes have a real part as

$$\omega_r = \frac{\epsilon\delta_T}{4}kv_{\text{th}}\cos\theta.$$

The imaginary part of the mode 1 is obtained as,

$$\gamma = \frac{\epsilon^2\delta_T^2}{8\sqrt{\pi}}kv_{\text{th}}(3\cos^2\theta - 2\sin^2\theta) - \frac{1}{\sqrt{\pi}}\left(\frac{c}{\omega_p}\right)^2 k^3v_{\text{th}},$$

and the imaginary part of the mode 2 is obtained as,

$$\gamma = \frac{3\epsilon^2\delta_T^2}{8\sqrt{\pi}}kv_{\text{th}}\cos^2\theta - \frac{1}{\sqrt{\pi}}\left(\frac{c}{\omega_p}\right)^2 k^3v_{\text{th}},$$

where  $\omega_p$  is the electron plasma frequency,  $c$  is the speed of light and  $\theta$  is the angle between the direction of the temperature gradient and the wave vector. The existence of the real part in the dispersion relation of the RL instability is one of the difference from the Weibel case. Since the phase velocity along the temperature gradient  $\omega_r/k\cos\theta = \frac{\epsilon\delta_T}{4}v_{\text{th}}$  only takes a positive value, the wave propagates only one way from the low temperature region to the high temperature region. Therefore, the excited waves do not carry the heat from the hot to the cold region. Although the mode 2 is a pure transverse wave, the longitudinal component of the electric fields,  $E_k$ , has a non-zero value for the mode 1 as

$$E_k \sim \frac{\epsilon\delta_T}{4}\sin\theta\frac{v_{\text{th}}}{c}B_z.$$

This is an another prominent difference from the Weibel case. The wave grows the most rapidly when the wave vector is parallel to the temperature gradient. The wave is damped when the direction of the wave propagation is perpendicular to the temperature gradient. The dependence on the  $k$  of the growth rate is the same as that of the Weibel.

In a sence that the anisotropic velocity distribution is the driving force of the instability, the both instabilities are similar and therefore the RL instability was said to be the Weibel like. However, there are plenty of the qualitative differences among the both instabilities as explained in above. Therefore, the both instabilities were distinguished (Gallev & Natanzon 1991) and we try to identify the physical mechanism of the RL instability in the next section.

#### 4. THE PHYSICAL MECHANISM OF THE RL INSTABILITY

The physical mechanism of the RL instability can be understood from the nature of the velocity distribution function when the finite heat flow exists, as illustrated in Figure 2. In

the following discussion, strictness of the numerical factor is ignored. The peak position is shifted toward positive  $v_{\parallel}$  direction and the amount of the shift is  $v_{\parallel} \sim \epsilon \delta_T v_{\text{th}}$ . The phase velocity of any low frequency magnetic transverse wave must be close to the velocity at where the distribution function has a peak value otherwise a finite net electric current is induced by the wave magnetic fields. This explains why the excited waves by the RL instability have the phase velocity of  $\epsilon \delta_T v_{\text{th}}$ , and travel one way direction rising up the temperature gradient and the waves can not travel in the direction of the perpendicular to the temperature gradient. The reason why the excited waves by the Weibel instability are standing wave, is simply because there is no shift in peak position of the velocity distribution function in the Weibel case. The peak value is increased by  $\sim 1 + (\epsilon \delta_T)^2$  from that of the pure Maxwell-Boltzmann case since the amplitude of the deviated part takes a value of  $\epsilon \delta_T v_{\parallel} \sim (\epsilon \delta_T)^2 v_{\text{th}}$  relative to the Maxwell-Boltzmann and the value of the Maxwell-Boltzmann part is nearly same as the peak value at  $v_{\parallel} \sim \epsilon \delta_T v_{\text{th}} \ll v_{\text{th}}$ . Since the total electron number density must be unchanged, for the observer comoving with the waves this can be interpreted as the decrease of the effective electron temperature in the direction of the temperature gradient,  $T_{\parallel}$ , by  $\sim 1 - (\epsilon \delta_T)^2$  relative to the temperature perpendicular to the temperature gradient,  $T_{\perp}$  (Fig.2). The growth of the magnetic waves in the RL instability is, therefore, due to essentially the same mechanism as the Weibel instability (Weibel 1959; Fried 1959) in which the temperature anisotropy is the driving force of the instability. Consider the waves traveling nearly parallel to the temperature gradient. In this case,  $T_{\perp, \vec{k}} \sim T_{\perp}$  and  $T_{\parallel, \vec{k}} \sim T_{\parallel}$  where  $T_{\perp, \vec{k}}$  and  $T_{\parallel, \vec{k}}$  are the temperature components perpendicular and parallel to the wave vector for the observers comoving with the waves, respectively. Since  $T_{\perp, \vec{k}} > T_{\parallel, \vec{k}}$ , the waves can grow. As a result, the direction of the magnetic field generated by the instability is almost perpendicular to the temperature gradient. The growth rate of the mode which travels toward the direction of the temperature gradient with wavenumber  $k$  is obtained from that of the Weibel instability (Krall 1973),

$$\begin{aligned} \gamma &\sim v_{\text{th}} \left[ \left( \frac{T_{\perp}}{T_{\parallel}} - 1 \right) k - \left( \frac{ck}{\omega_p} \right)^2 k \right] \\ &\sim v_{\text{th}} \left[ (\epsilon \delta_T)^2 k - \left( \frac{ck}{\omega_p} \right)^2 k \right]. \end{aligned}$$

The growth rate gets the maximum value of  $\gamma_{\text{max}} \sim (\epsilon \delta_T)^3 (v_{\text{th}}/c) \omega_p$  at  $k = k_{\text{max}} \sim \epsilon \delta_T \omega_p / c$ . When the direction of the wave vector is perpendicular to the temperature gradient,  $T_{\perp, \vec{k}} = T_{\parallel}$  and  $T_{\parallel, \vec{k}} = T_{\perp}$ . Since  $T_{\perp, \vec{k}} < T_{\parallel, \vec{k}}$  in this case, the wave can not grow. These results are exactly the same as the results led by the plasma kinetic theory except numerical factors (Ramani & Laval 1978; Hattori & Umetsu 2000; Okabe & Hattori in preparation).

The above discussion gives a complete physical explanation for the mode 2 of the RL in-

stability. However, these are not satisfactory to the mode 1 in which the longitudinal electric field component appears. Unfortunately, we have not yet gotten the physical explanation for this. This is still an open question.

## 5. ON THE NONLINEAR EVOLUTIONS OF THE RL INSTABILITY

The nonlinear saturation level of the excited wave is estimated assuming that the wave-particle interaction determines the saturation level. The fundamentals are illustrated in Figure 3 (Ramani & Laval 1978; Gallev & Natanzon 1991). Once the Larmor radius of an electron gets shorter than the wavelength of the growing mode, the electron is trapped by the magnetic field of the wave and the magnetic flux enclosed by its orbit becomes finite. Then, the kinetic energy of the trapped electron starts monotonically increase as the growth of the magnetic field strength, since the increase of the magnetic flux enclosed by the electron orbit cause the induction electric fields which accelerate the electron as the betatron accelerator. Once the Larmor radius of typical thermal electrons,  $r_L \sim v_{th}\omega_c^{-1}$ , gets shorter than the wavelength of the fastest growing mode, that is  $r_L k_{max} < 1$ , the increase of the kinetic energy of the electron system becomes significant if the waves still continue to grow. Since this finally violates the energy conservation, the growth of the magnetic field strength must be saturated when  $r_L k_{max} \sim 1$ .

The evolution of the magnetic fields after the nonlinear saturation could be described as follows. Some numerical simulations which follow the evolution of the Weibel instability, showed that the strength of the magnetic field driven by the Weibel instability decreases after it gets the maximum value (Morse & Nielson 1971). This can be understood as follows. As the magnetic field grows, the electron velocity distribution is isotropitized and it becomes difficult to maintain the electric current field which supports the magnetic field of the waves. In these simulations, the system is assumed to be isolated and the initial anisotropic velocity distribution function let be free to evolve to isotropic one. On the other hand, in the case of the RL instability there is a driving force which maintains the anisotropy of the velocity distribution function. As far as the temperature gradient is not disappeared, the finite heat flux transports the heat from the hot to the cold region and the anisotropic velocity distribution function discussed in section 2 is maintained. Therefore, the decrease of the magnetic field strength after the nonlinear saturation as found in the Weibel instability may not be occurred in the RL instability. It is expected that the generated magnetic field strength is kept to be the saturated value for the life time of the temperature gradient. Wallace and Epperlein (1991) performed the numerical simulations to follow the evolution of the Weibel instability when an initial anisotropic distribution function is maintained by

an external source. They showed that the magnetic field strength is kept constant value after the saturation. Their results support the above expectation for the RL instability. There are several indicative numerical simulations concerning the organization of the globally connected magnetic fields from the wavy fields generated by the instability. The wavy magnetic fields generated by the Weibel instability evolve into the longer wavelength modes after the saturation (Lee 1973; Sentoku et al. 2000; Sentoku et al. 2002). This result indicates that the excited wavy magnetic field automatically evolves into the globally connected fields. This could be understood as follows. After the magnetic field strength gets the saturated level, the electric current field starts to play as an individual electric beams every half wave length (Fig.4). Each beam is surrounded by the azimuthal magnetic field generated by the current beam itself. The electric beams interact each other via the Ampère’s force (Sentoku et al. 2000; Sentoku et al. 2002). The beams directed to the same direction are attracted each other and automatically gather. Finally, they merge into larger one beam. Since the physical mechanism of the growth of the RL instability is the same as the Weibel instability as shown in section 4, the same evolution is expected even in the RL case.

Although the reduction of the heat conductivity was originally considered due to the electrons scattering by the waves generated by the RL instability (Ramani & Laval 1978; Hattori & Umetsu 2000), this may not be the case. As discussed in above, the wavy magnetic field generated by the instability could tend to form the global magnetic field automatically. Therefore, the suppression of the heat conductivity may be determined by the trapping of the electrons by the organized magnetic field. To estimate the suppression of the heat conductivity quantitatively, we have to know what is the final structure of the magnetic field due to the self-organization. The detail nonlinear studies, numerical simulations for example, are desired to answer the questions.

## 6. APPLICATION TO THE COLD FRONT IN A3667

The above results are applied to the cold front found in the cluster of galaxies A3667. The temperature and density of the electron changes from  $k_B T_c = 4.1 \pm 0.2$  keV and  $n_{e,c} = 3.2 \pm 0.5 \times 10^{-3}$  cm $^{-3}$  to  $k_B T_h = 7.7 \pm 0.8$  keV and  $n_{e,h} = 0.82 \pm 0.12 \times 10^{-3}$  cm $^{-3}$  across the cold front (Vikhlinin, Markevitch & Murray 2001a). The width of cold front is  $L \sim 5$  kpc at maximum. The Coulomb mean free path of the thermal electron in the cold front region is  $\lambda_e = 5.4(T/T_{\text{ave}})^2(n_e/n_{\text{ave}})^{-1}$  kpc where  $T_{\text{ave}} = (T_h + T_c)/2$  and  $n_{\text{ave}} = (n_{e,h} + n_{e,c})/2$ . Thus,  $\epsilon\delta_T \sim 1$  in the cold front of A3367. The growth time scale of the unstable mode in the cold front is  $\gamma_{\text{max}}^{-1} \sim 0.1$ sec. Although the exact time scale over which the instability can generate magnetic fields with the saturation values over the scale of the



interfaces is difficult to estimate, that must be several tens times longer than the growth time scale. Therefore, it is expected that the magnetic field is generated almost instantaneously compared with any other dynamical time scales in the cluster of galaxies. By applying the saturation level discussed in the previous section, the saturated magnetic field strength in the cold front should be  $B_{\text{sp},\perp} \sim \sqrt{\pi} \sqrt{n_e k_B T} \epsilon \delta_T \simeq 8 (T/T_{\text{ave}})^{3/2} (n/n_{\text{ave}})^{-1/2} \mu\text{G}$  where the exact dispersion relation obtained by Ramani and Laval (1978) was used. The obtained value agrees surprisingly well with the speculated value of  $10 \mu\text{G}$  based on the stability consideration against the KH instability. The direction of the generated magnetic field should be almost parallel to the cold front surface due to the characteristics of the mode. As discussed in section 5, the generated wavy magnetic fields could tend to evolve into the globally connected field. Therefore, we expect that the cold front surface is covered by the globally connected magnetic fields directed tangential to the surface with the strength of  $10 \mu\text{G}$  and the KH instability is suppressed by these fields. Although to suppress the KH instability the existence of the magnetic fields are required only in the tail of the cold fronts (Vikhlinin, Markevitch & Murray 2001b), our model predicts the existence of such a strong fields all over the cold front where the temperature jump exists. The generated magnetic field may significantly reduce the electron mean free path in the direction of the temperature gradient and could suppress the heat conduction all over the cold fronts.

## 7. DISCUSSION

We have successfully determined the physical mechanism responsible for one of the two independent modes of the RL instability, and shown that the growth mechanism is identical to the Weibel instability which is well-known as one of the generation mechanism of the magnetic field. Therefore, the RL instability can be also considered as the generation mechanism of the magnetic fields in the astronomical situations. The nonlinear saturation level of the instability is estimated by considering the wave-particle interaction. The evolutions of the magnetic fields after the saturation are speculated by referring the previous numerical simulations which followed the non-linear evolution of the Weibel instability. The generated fields might be self-organized and evolve into the globally connected magnetic field. The results are applied to the cold front in A3667. The existence of the magnetic field of  $\sim 10 \mu\text{G}$  tangential to the surfaces in all over the cold front is predicted. The results surprisingly agree with the predicted nature of the magnetic field in the cold front to explain the smoothness of the cold front surface structure avoiding the KH instability. Although the suppression of the KH instability requires the existence of the strong magnetic field only in the tail of the cold front, our model predicts the existence of such a strong fields all over the cold front where the temperature jump exists. The significant suppression of the heat conduction in

the cold front is also expected by the trapping of the electrons by the generated magnetic fields. Thus, our model predicts that the bow-shaped structure of the cold fronts should not partially disappear and the whole structure should be maintained.

Of course further studies on the RL instability are desired. The non-linear studies using the numerical simulations specificated to the RL instability and the cold front are one of the most important remaining subjects. The identification of the physical mechanism of the mode 1 how the longitudinal electric field is generated, is another important remained subject.

The physics of the RL instability discussed in this paper should be universal and the RL instability may play an important role in various hot thin plasmas in the universe. For example, the temperature inhomogeneities of  $\epsilon\delta_T \sim 0.04$  distributed in whole cluster has been found in almost all clusters of galaxies. The RL instability predicts the existence of the cluster halo magnetic field with strength of  $B \sim 0.04 \times \sqrt{n_e k_B T} \sim 0.3\mu\text{G}$ . Surprisingly the predicted value just coincides with the observationally reported cluster halo magnetic field strength. The details of this topic are reported in the force coming paper (Okabe & Hattori in preparation). We believe that the RL instability may provide a new fruitful possibility on the origin of the cosmic magnetic field.

### Acknowledgments

The authors gratefully thank T. N. Kato, M. Iijima, M. Takizawa, H. Ohno and Y. Fujita for their a lot of fruitful comments, and anonymous referee for one's constructive comments.

### A. Appendix : THE WEIBEL INSTABILITY

The Weibel instability is driven by an anisotropic temperature distribution and generates the growing transverse magnetic standing waves (Weibel 1959). This instability is well-known as the mechanism of the magnetic fields generation from zero initial magnetic field. Consider the plasma with an anisotropic temperature such as

$$f = n_0 \frac{1}{\pi^{3/2} v_{\text{th},\perp}^2 v_{\text{th},\parallel}} \exp \left[ -\frac{v_{\parallel}^2}{v_{\text{th},\parallel}^2} - \frac{v_{\perp}^2}{v_{\text{th},\perp}^2} \right],$$

where the subscripts  $\parallel, \perp$  respectively denote the parallel and perpendicular direction to the wave vector. The dispersion relation is obtained by the linear plasma kinetic theory

(Krall 1973) as

$$\begin{aligned}\omega_r &= 0, \\ \gamma &= \frac{1}{\sqrt{\pi}} k v_{\text{th},\parallel} \frac{T_{\parallel}}{T_{\perp}} \left[ \left( \frac{T_{\perp}}{T_{\parallel}} - 1 \right) - \left( \frac{kc}{\omega_p} \right)^2 \right].\end{aligned}$$

The waves has no real part of the frequency. The waves grow when  $T_{\perp} > T_{\parallel}$ . The excited waves are transverse magnetic waves with no electric field.

The physical mechanism of the Weibel instability is first identified by Fried (1959). Consider the simple situations as shown in Fig. 4. The electrons and their initial velocities are expressed as the filled circles and the dotted arrows. In the case A, the simple anisotropic initial electron distribution function

$$f_0(\vec{v}) = n_0 u \delta(v_{\parallel}) \delta(v_{\perp}^2 - u^2) \delta(v_z)$$

is assumed where  $n_0$  is the electron number density. This represents an extreme case of  $T_{\perp} \neq 0, T_{\parallel} = 0$ . In the case B, the anisotropic initial electron distribution function

$$f_0(\vec{v}) = n_0 w \delta(v_{\parallel}^2 - w^2) \delta(v_{\perp}) \delta(v_z)$$

is assumed. This represents an extreme case of  $T_{\perp} = 0, T_{\parallel} \neq 0$ . The directions of the perturbed magnetic fields are perpendicular to the paper :  $\odot$  &  $\otimes$  represent that the fields project from the paper and rush in the paper, respectively. The size of the circle is proportional to the field strength at each position.

Firstly, the qualitative explanation of the physical mechanism is reviewed. The electrons' orbits are deflected due to the introduction of the perturbed magnetic field as shown by the dashed arrows. The amount of the deflection is proportional to the field strengths at the each position. We first discuss the Case A. Consider the electrons (a) and (a') which initially have the negative velocity in the  $x_{\perp}$  direction. They respectively carry the positive electric currents in the  $x_{\perp}$  direction out from and into the shaded region. Because of the difference of the field strengths, the net positive current in the  $x_{\perp}$  direction is carried out from the region in a certain infinitesimal time interval. In other words the net negative electric current is carried into the region by the perturbed motion of these electrons. The electrons (b) and (b') also carry the net negative electric current into the shaded region. Therefore, the net negative electric current is developed in the shaded region due to the injection of the perturbed magnetic field. Since the values of the induced electric currents are larger where the gradient of the magnetic field strength is larger, the current fields illustrated in Fig. 4 are set up where the length of the arrows are proportional to the amplitudes of the currents. The magnetic field is produced around each electric current according to the Ampère's law

as illustrated in Fig.4. The growth of the magnetic field is determined by the superposition of these fields. For example, at point  $x_1$  the net magnetic field generated by the current fields is normal to the paper toward readers and amplifies the injected perturbed field. Since the excited fields amplify the injected perturbed fields everywhere, the perturbed field grows in the Case A. On the other hand, the net induced electric currents direct opposite direction to Case A in the Case B. Therefore, the perturbed magnetic field is damped in the Case B. Hence, when  $u > w$  ( $T_\perp > T_\parallel$ ) the magnetic field perturbation grows and when  $u < w$  ( $T_\perp < T_\parallel$ ) the magnetic field perturbation is damped. While this simple explanation shows qualitatively how the growth occurs, the role of the electromagnetic induction for the growth of the instability, which was neglected in the above discussion, should be examined since it acts to reduce the growth of the magnetic field.

Next, the semi quantitative explanation of the instability is given to see the role of the induction. For this purpose, only the case A is considered. Suppose that an initial perturbed magnetic field is

$$B_z = B e^{ikx_\parallel}.$$

The  $x_\parallel$  and  $x_\perp$  components of the equation of motion of the electron are given by

$$\begin{aligned} m_e \frac{dv_\parallel}{dt} &= -e \frac{v_\perp}{c} B_z, \\ m_e \frac{dv_\perp}{dt} &= e \frac{v_\parallel}{c} B_z - \frac{ie}{kc} \frac{\partial B_z}{\partial t}, \end{aligned}$$

respectively, where the last term in  $x_\perp$  component represents the force due to the inductive electric field. Therefore, the time derivative of the electric current flux is given by

$$\frac{\partial \langle j_\perp v_\parallel \rangle}{\partial t} = e^2 \frac{u^2}{cm_e} B_z,$$

where  $j_\perp = -ev_\perp$  is the  $x_\perp$  component of the electric current carried by an single electron and  $\langle X \rangle = \frac{1}{n_0} \int d^3v X(v) f(v)$  is the average over the velocity space. This current flux and the inductive electric field cause a change in the mean value of  $j_\perp$  as

$$\frac{\partial \langle j_\perp \rangle}{\partial t} = -\frac{\partial \langle j_\perp v_\parallel \rangle}{\partial x_\parallel} + e^2 i \frac{1}{m_e kc} \frac{\partial B_z}{\partial t}.$$

The Ampère's law provides

$$n_0 \langle j_\perp \rangle = -\frac{ick}{4\pi} B_z,$$

where the displacement current is neglected since the low frequency mode is only considered. By combining these equations, we obtain

$$\left[1 + \frac{\omega_p^2}{c^2 k^2}\right] \frac{\partial^2 B_z}{\partial t^2} = \frac{\omega_p^2}{c^2} u^2 B_z.$$

The dispersion relation is obtained as

$$\gamma = \frac{(\omega_p/c)u}{\sqrt{1 + \frac{\omega_p^2}{c^2 k^2}}}.$$

It shows that the perturbation can grow. The second term in the [ ] of the left hand side is coming from the induction term. Therefore, the electromagnetic induction actually plays a role of the inertia for the growth of the perturbation and reduces the growth rate, but never stop the growth of the perturbation. The obtained growth rate is exactly the same as the result deduced by the full linear analysis based on the plasma kinetic theory where the induction effect is also taken into account (e.g. Melrose 1986).

## REFERENCES

- Chapman, S. & Cowling, T. G. 1960, *The Mathematical Theory of Nonuniform Gases* (Cambridge: Cambridge Univ. Press)
- Ettori, S. & Fabian, A. C. 2000, *MNRAS*, 317, L57
- Fried, B. D. 1959, *Phys. Fluids*. 2, 337
- Gallev, A. A. & Natanzon, A. M. 1991, *Physics of laser plasma* Chap 13 (eds Rubenchik, A. & Witkowski, S., Amsterdam ; Tokyo : North-Holland)
- Hattori, M. & Umetsu, K. 2000, *ApJ*, 533, 84
- Kato, T., private communication & in preparation
- Krall, A. & Trivelpiece, A. W. 1973, *Principles of plasma physics* (New York: McGraw-Hill)
- Lee, R & Lampe, M. 1973, *Phy. Rev. Lett.*, 31, 1390
- Levinson, A. & Eichler, D. 1992, *ApJ*, 387, 212
- Markevitch, M., Ponman, T. J., Nulsen, P. E. J., Bautz, M. W., Burke, D. J., David, L. P., Davis, D., Donnelly, R. H., Forman, W. R., Jones, C., Kaastra, J., Kellogg, E., Kim, D.-W., Kolodziejczak, J., Mazzotta, P., Pagliaro, A., Patel, S., Van Speybroeck, L., Vikhlinin, A., Vrtilik, J., Wise, M., & Zhao, P. 2000, *ApJ*, 541, 542

- Melrose D.B. 1986, *Instabilities in Space and Laboratory Plasmas* (Cambridge: Cambridge Univ. Press)
- Morse R. L. & Nielson C. W. 1971, *Phys. Fluids.*, 14, 830
- Okabe, N. & Hattori, M., in preparation.
- Ramani, A. & Laval, G. 1978, *Phys. Fluids.*, 21, 980
- Sarazin, C. L. 1988, *X-ray emission from the Clusters of Galaxies* (Cambridge: Cambridge Univ. Press)
- Sentoku, Y., Mima, K., Kojima, S., Ruhl, H., 2000, *Phys. Plasma*, 7, 689
- Sentoku, Y., Mima, K., Sheng, Z. M., Kaw, P., Nishihara, K. & Nishihara, K. 2002, *Phys. Rev. E.*, 65, 046408
- Vikhlinin, A., Markevitch, M. & Murray, S. S. 2001a, *ApJ*, 551, 160
- Vikhlinin, A., Markevitch, M. & Murray, S. S. 2001b, *ApJ*, 549, L47
- Vikhlinin, A. & Markevitch, M. 2002, *AstL*, 28, 495
- Weibel, E. S. 1959, *Phys. Rev. Lett.*, 2, 83
- Wallace, J. M. & Epperlein, E. M. 1991, *Phys. Fluids B*, 3, 1579

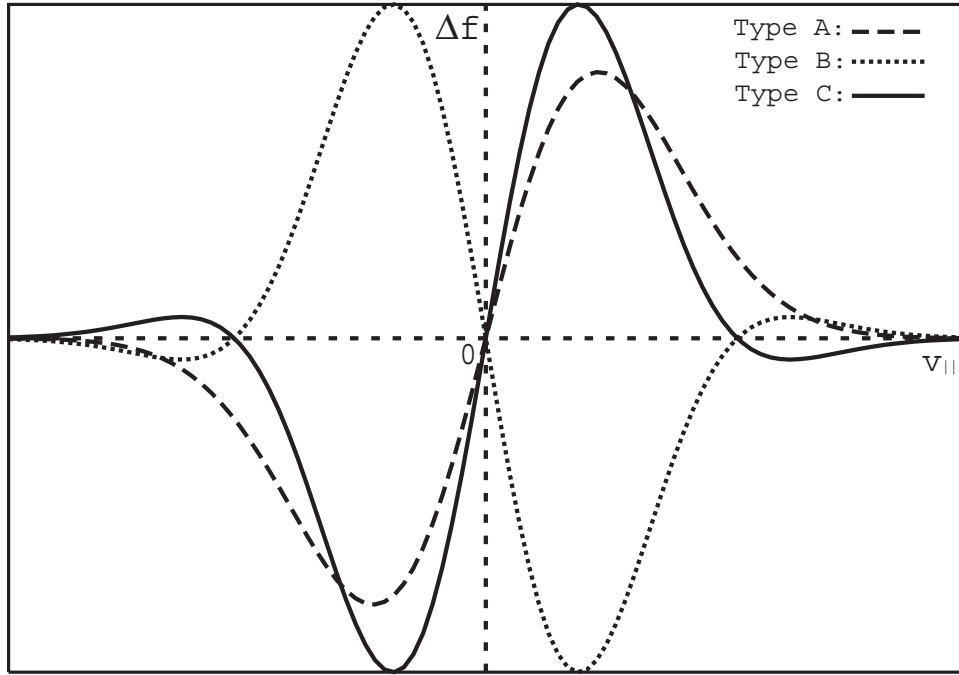


Fig. 1.— The possible candidates as the deviated part of the velocity distribution function from the Maxwell-Boltzmann.

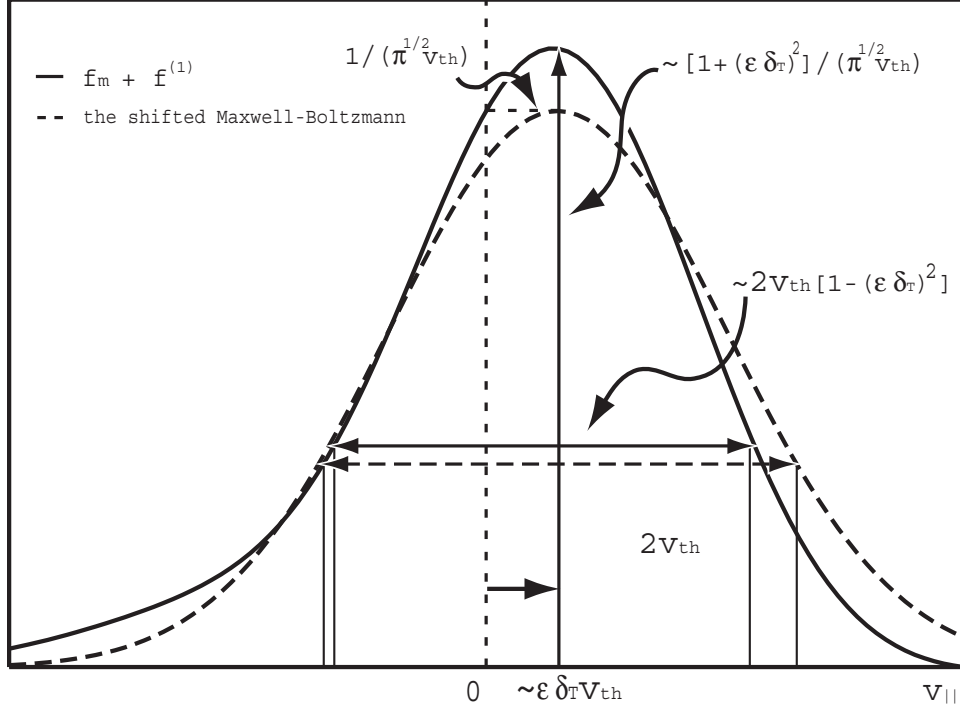


Fig. 2.— The solid line is the  $v_{||}$  section of the total velocity distribution function  $f_m + f^{(1)}$  in the plasma with the temperature gradient. The peak position is shifted by  $\sim \epsilon \delta_T v_{th}$  from the Maxwell-Boltzmann. The peak value is increased by  $\sim 1 + \epsilon^2 \delta_T^2$  compared with the Maxwell-Boltzmann. For comparison, the Maxwell-Boltzmann velocity distribution function shifted by  $\sim \epsilon \delta_T v_{th}$  drawn in the dashed line. The velocity distribution function gets thinner in  $v_{||}$  direction. This can be interpreted as the decrease of the effective temperature by  $\sim 1 - \epsilon^2 \delta_T^2$  in the direction of the temperature gradient.



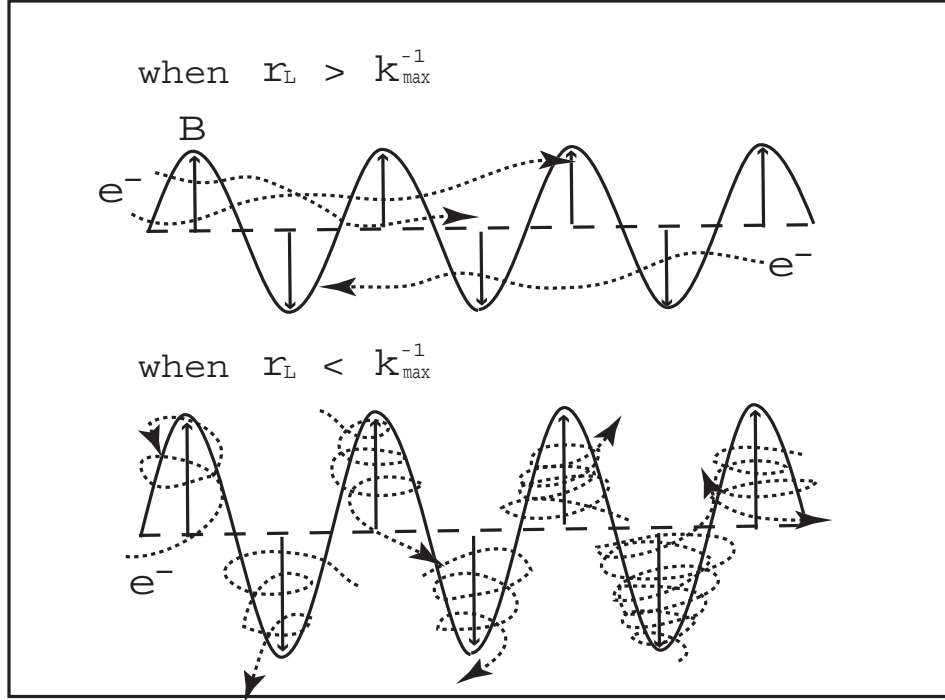


Fig. 3.— The nonlinear saturation by the wave-particle interaction. The top panel: When  $r_L > k_{\max}^{-1}$ , the thermal electrons travel throughout the waves but their orbits are randomly disturbed by the wavy magnetic fields. The bottom panel: Once  $r_L$  becomes smaller than  $k_{\max}^{-1}$ , the thermal electrons are trapped by the fields and feels net non zero fields.

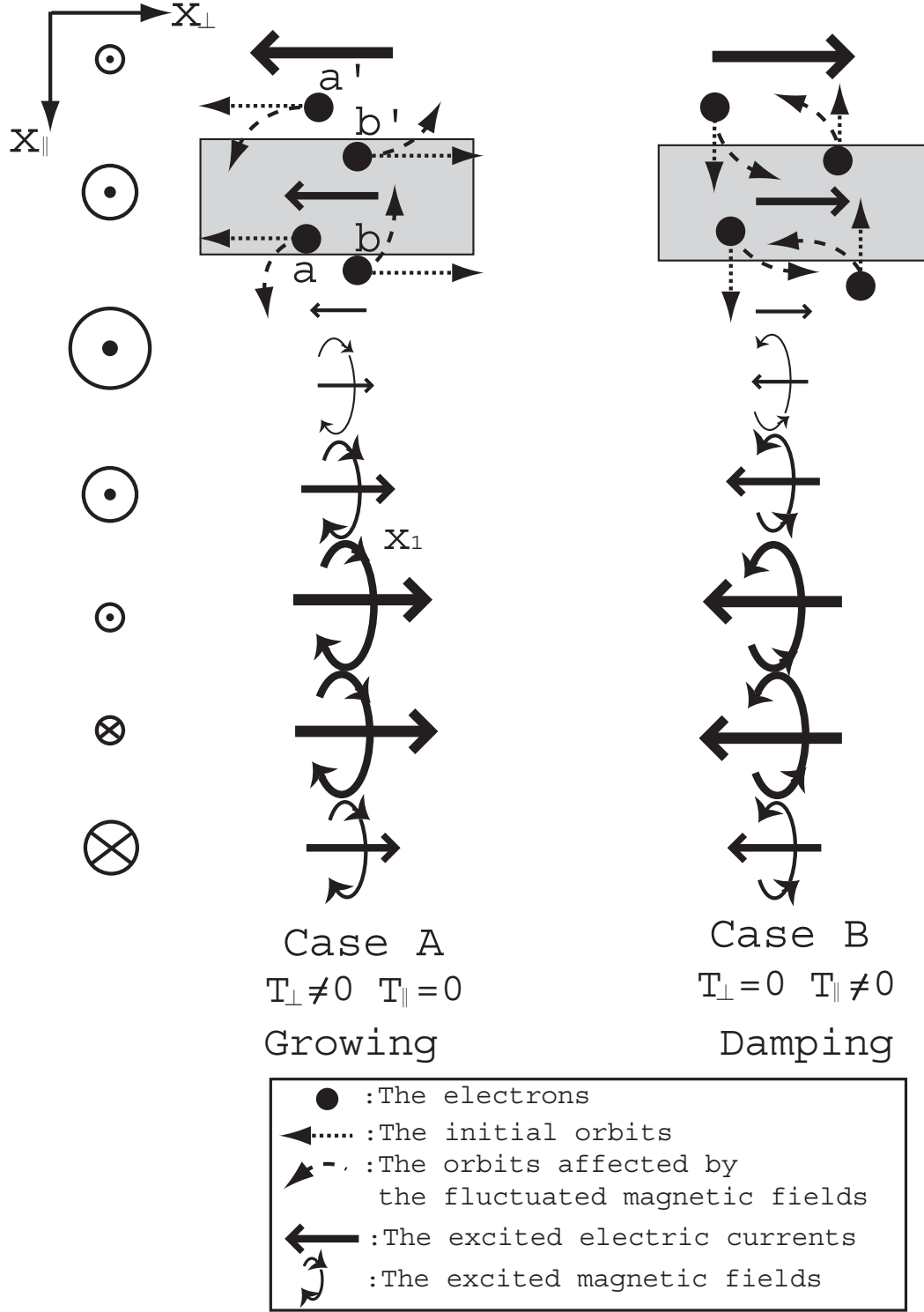


Fig. 4.— The physical mechanism of the Weibel instability